

## Correlation between Thermal Expansion and Magnetic Characteristics of Fe-Ni Alloys in $\text{Fe}_{1-x}\text{Ni}_x/\text{Cu}$ Superlattices

Weizhong Tang<sup>1)</sup>, H Zabel<sup>2)</sup>

1) Material Science and Engineering School, University of Science and Technology Beijing, Beijing 100083, China

2) Institute of Experimental Physics/Solid State Physics, Ruhr University Bochum, 44780 Bochum, Germany

(Received 1998-04-28)

**Abstract:** Thermal expansion behaviors of FeNi alloys were investigated by means of X-ray diffraction technique within a  $\text{Fe}_{1-x}\text{Ni}_x/\text{Cu}$  superlattice structure. It was found that with a Ni concentration of  $x = 0.35$ , FeNi alloy layers showed the well-known Invar behavior, but for alloy layers with either lower or higher Ni concentrations, thermal expansion coefficients were larger. Based on results of magnetic measurements it is concluded that FeNi alloy layers with Ni concentrations lower than the Invar composition are in a superparamagnetic state which leads not only to low spontaneous magnetizations but also to large thermal expansions of the alloy layers.

**Key words:** thermal expansion; Invar behavior; FeNi alloys; superlattice; magnetism

Fe-Ni alloys exhibit not only novel low thermal expansion properties at around room temperature, but also unusual magnetic behaviors. For example, near the composition of a typical Invar alloy (with a Ni concentration (atom fraction, so as followed) of about 35%), the mean magnetic moment of an atom within the alloy deviates from the well-known Slater-Pauling curve [1]. Theoretical explanations for such abnormal behaviors include the early  $2\gamma$ -state assumption [2] and the recently developed Moment-Volume-Instability (MVI) theory [3]. According to these models there exist two magnetically ordered states, either local or itinerant, all with the face-centered cubic (f.c.c.) crystal structure. The ferromagnetic state corresponds to a large atomic volume, and the nonferromagnetic state has an atomic volume somewhat smaller. While the two states are energetically different, the latter can be thermally excited and thus will compensate the ordinary lattice expansions associated with phonon excitations. Based on either of these models, one would expect that a rapid decline in spontaneous magnetization of a FeNi alloy with increasing temperature would be accompanied by a low thermal expansion rate, and such an abnormal thermal expansion should be observable in all f.c.c. Fe-Ni alloys in which the energy gaps between the ferro- and the non-ferromagnetic states are small.

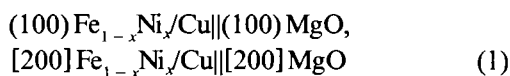
Experimentally, f.c.c. FeNi alloys of Invar composition do show low thermal expansion rate in addition to rapid declines in spontaneous magnetization with increasing temperature. But for FeNi alloys with even lower Ni concentrations, it is difficult to correlate their magnetic characteristics to thermal expansion properties. The reason for this difficulty is that these alloys, if they were to be prepared in bulk forms, would transform to a body-centered-cubic (b.c.c.) crystal structure when temperature drops below room temperature. Specifically, though theoretical calculations have predicted that FeNi alloys with Ni concentrations around 25% should possess low thermal expansion abnormality [4-6], the f.c.c. to b.c.c. phase transformation has prevented from experimental determination of thermal expansion behaviors of such low Ni alloys at low temperatures. At high temperatures, an anti-Invar behavior (an abnormally higher than normal thermal expansion) has been observed in low Ni f.c.c. alloys. But unfortunately, in such conditions, the alloys would be in a paramagnetic state [7].

Recently, f.c.c. structured FeNi/Cu superlattices with FeNi alloy layers of Ni concentration as low as 26% have been prepared, and the epitaxial relationship between the FeNi and Cu sublayers extended the stability of f.c.c. crystal structure of the alloys even down to liquid helium temperatures [8]. With such

novel structures it is possible to further the investigation on thermal expansion behaviors of f. c. c. FeNi alloys into low Ni concentrations. This paper reports on experimental results of thermal expansion properties of FeNi alloy layers within the FeNi/Cu superlattices and the correlation between thermal expansion behaviors of such alloy layers and their magnetic characteristics will be discussed.

## 1 Experimental

F. c. c.  $[(\text{Fe}_{1-x}\text{Ni}_x)_{3\text{nm}}\text{Cu}_{3\text{nm}}] \times 10$  superlattices ( $x = 0.26\text{--}0.54$ ) were sputter deposited on MgO(100) substrates as described before [8]. The sputtering procedure was begun and then completed with the deposition of Cu layers, to ensure the epitaxial growth of the superlattices on the substrates and to protect the superlattices from oxidation. The epitaxial relationship of the superlattices has been revealed by X-ray diffraction as



For comparison, a single layer Cu film was also epitaxially deposited with a comparable total film thickness (about 60 nm).

Out-of-plane X-ray diffraction measurements were undertaken to measure the thermal expansion behaviors of the superlattices along the direction normal to the superlattice plane. Cu- $K_\alpha$  radiation was selected for the diffraction measurements. The measurements spanned 10–300 K by using a cryostat. The diffraction curves were numerically fitted to deduce out-of-plane lattice parameters, as will be described below.

Magnetic measurements were undertaken using a vibrating sample magnetometer and a Faraday balance. The detailed description of these measurements has been given before [8].

## 2 Results and Discussion

In figure 1 are shown the (002) diffraction curves of three  $\text{Fe}_{1-x}\text{Ni}_x/\text{Cu}$  superlattices measured at different temperatures. It is seen that in addition to the primary Bragg peaks at about  $50.5^\circ$ , there are small superlattice satellites of varying intensities. The intensities of the satellites on the small angle side are higher than those on the large angle side, indicating that in the superlattices the Cu sublayers with a little larger atomic scattering ability have an out-of-plane lattice parameter larger than that of the FeNi sublayers. The

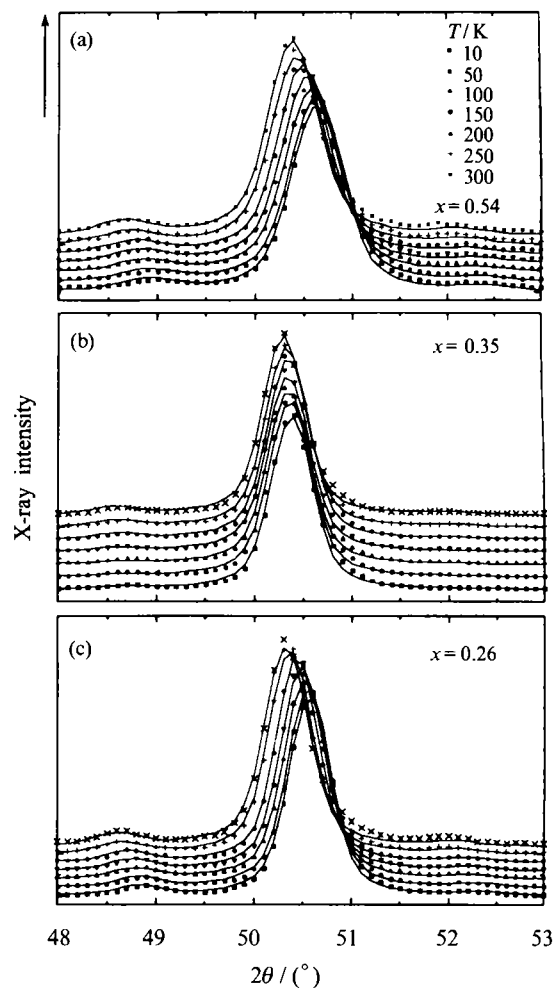


Figure 1 X-ray diffraction curves of three  $\text{Fe}_{1-x}\text{Ni}_x/\text{Cu}$  superlattices at different temperatures (points) and corresponding fitted curves. The curves for successive temperatures have been displaced vertically for the reason of clarity

linewidth of the diffraction peaks is independent of temperature, confirming that the coherence length of these superlattices in the out-of-plane direction remains the same during the temperature cycling, and the phase transformation from f. c. c. to b. c. c. crystal structure is inhibited by the epitaxy.

As temperature increases, the Bragg peaks of these superlattices move towards small angles due to thermal expansions in the out-of-plane direction. For the superlattice with a Ni concentration of  $x = 0.35$ , this movement is rather small, consistent with the Invar behavior found in corresponding bulk FeNi alloys.

By assuming a single Gaussian lineshape profile, the (002) diffraction peaks in figure 1 were fitted to deduce the averaged lattice parameter,  $\bar{a}$ , of the superlattices in the out-of-plane direction. Lattice parameters of both FeNi and Cu sublayers,  $a_{\text{FeNi}}$  and  $a_{\text{Cu}}$ ,

could be determined by numerically fitting the diffraction curves with a one-dimensional model assuming that the superlattices were composed of FeNi and Cu slabs with different coherence lengths. Using a formula similar to the one used in references [9] and [10], X-ray intensity at a diffraction angle  $\theta$  may be written as

$$I = I_0 L(\theta) p_n \sum_{N_1 < n < N_2} F_n^2 \quad (2)$$

where  $I_0$  is the intensity of incident X-ray beam,  $L(\theta)$  the Lorentz polarization factor,  $F_n$  the structure factor of  $n$  coherently arranged atom layers,  $p_n$  the probability of finding such a coherence length, and  $N_1$  and  $N_2$  the upper and lower limits for the summation, taking into account all the possible combinations of successive FeNi and Cu atom layers. The temperature dependence of atomic scattering factors was ignored, which

should only result in small errors in fitting results in a small diffraction angle range. On the other hand, no roughness at interfaces between FeNi and Cu sublayers was taken into account because actual fitting procedures proved that such roughness had only trivial effects on final fitting results.

In equation (2),  $p_n$  is assumed to obey a normal distribution function, with  $\bar{n}$  and  $\sigma$  two fitting parameters, where  $\bar{n}$  is the mean coherence length, and  $\sigma$  the standard deviation of the distribution, all in units of atom layers. For the calculation of  $F_n$ , atomic scattering factors for Fe, Ni and Cu were obtained from reference [11], and scattering factor of atoms in  $\text{Fe}_{1-x}\text{Ni}_x$  alloys is assumed to be the compositional average of those of Fe and Ni elements.

In table 1 are listed the structural characteristics of the  $\text{Fe}_{1-x}\text{Ni}_x/\text{Cu}$  superlattices at 300 K, obtained by

**Table 1** Fitting results of the  $\text{Fe}_{1-x}\text{Ni}_x/\text{Cu}$  superlattices and the epitaxial Cu single layer at 300 K

Sample	Ni content $x$	Out-of-plane lattice parameter / nm			Superlattice structural parameter (atom layer)			
		$\bar{a}$	$a_{\text{FeNi}}$	$a_{\text{Cu}}$	$\bar{n}$	$\sigma$	$n_{\text{FeNi}}$	$n_{\text{Cu}}$
$\text{Fe}_{1-x}\text{Ni}_x/\text{Cu}$ superlattice	0.54	0.362 15	0.357 91	0.365 63	38	43	14	17
	0.35	0.362 79	0.359 74	0.365 32	52	51	14	17
	0.26	0.362 53	0.358 72	0.365 68	50	47	14	17
Cu single layer	—	—	—	0.361 42	75	49	—	—

fitting the diffraction curves in figure 1. The numbers of atom layers within a single  $\text{Fe}_{1-x}\text{Ni}_x$  or Cu sublayers,  $n_{\text{FeNi}}$  and  $n_{\text{Cu}}$ , were determined to be 14 and 17, respectively. The superlattices have a coherence length of about 7–9 nm, along with a rather broad coherence length distribution.

The temperature dependence of both the averaged lattice parameter  $\bar{a}$  of the superlattices and the lattice parameters  $a_{\text{FeNi}}$  and  $a_{\text{Cu}}$  of the FeNi and Cu sublayers in the out-of-plane direction is shown in figure 2. From figure 2(a) it is seen that as the Ni content in the superlattices decreases, the temperature dependence of averaged lattice parameter  $\bar{a}$  changes in a complex way. Since there is always the same interlayer material Cu separating the FeNi alloy layers, the difference in the thermal expansion behavior of FeNi alloy layers should be the reason for such differences in  $\bar{a}$ . For a Ni concentration of 54%, an averaged thermal expansion coefficient of about  $19.4 \times 10^{-6}/\text{K}$  was obtained in 100–300 K. As the Ni concentration is decreased to 35%, a much lower thermal expansion coefficient is obtained which amounts to a value of  $5.5 \times 10^{-6}/\text{K}$  in the same temperature range. This is consistent with the

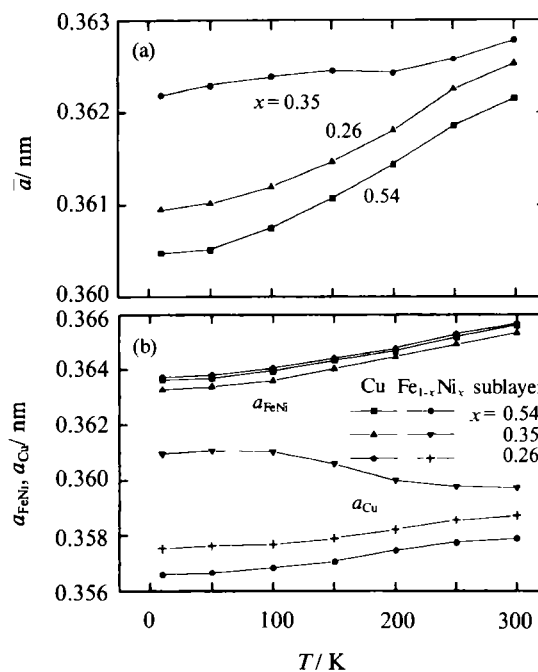


**Figure 2** Temperature dependence of (a) averaged out-of-plane lattice parameter  $\bar{a}$  of the three  $\text{Fe}_{1-x}\text{Ni}_x/\text{Cu}$  superlattices and (b) the lattice parameters  $a_{\text{FeNi}}$  and  $a_{\text{Cu}}$  for  $\text{Fe}_{1-x}\text{Ni}_x/\text{Cu}$  and Cu sublayers in the superlattices

Invar behavior of FeNi bulk alloys in which a nearly zero expansion behavior is attributed to the moment-volume-instability. As the Ni concentration in the FeNi alloy layers is further decreased to 26%, the averaged thermal expansion coefficient increases again to  $18.4 \times 10^{-6}/\text{K}$ , a value comparable to that of the superlattice with a Ni concentration of 54%.

From figure 2(b) it could be seen more clearly that the differences in temperature dependence of averaged lattice parameter  $\bar{a}$  is indeed due to the difference in the thermal behavior of FeNi sublayers. At 300 K, Cu sublayers have lattice parameters ranging from 0.3653 to 0.3657 nm, while FeNi sublayers show large differences in lattice parameters ranging from 0.3579 to 0.3597 nm, dependent on the Ni concentrations of the sublayers. While Cu sublayers in the three superlattices expand almost the same with increasing temperature, reaching a value for the expansion coefficient of  $(23\sim 24) \times 10^{-6}/\text{K}$  in 100~300 K, the thermal expansion of the FeNi sublayers is very different from one superlattice to another, and the averaged thermal expansion coefficients reach  $14.8 \times 10^{-6}$ ,  $-17.9 \times 10^{-6}$  and  $14.5 \times 10^{-6}/\text{K}$  for  $x = 0.54$ , 0.35 and 0.26, respectively. A negative thermal expansion is obtained for the FeNi sublayers with the Invar composition ( $x = 0.35$ ) in the temperature range of 100~300 K, and for the lowest Ni composition ( $x = 0.26$ ), a large positive thermal expansion comparable to that of FeNi sublayers with Ni concentration of  $x = 0.54$  is confirmed.

In interpreting above thermal expansion behaviors of superlattices, not only the constitutional materials, but also their clamping to the substrates should be taken into account. To verify this point of view, figure 3(a) shows (002) diffraction curves of the Cu single layer film epitaxially deposited on an MgO(100) substrate. The structural characteristics of this Cu film at 300 K are also included in table 1, and the out-of-plane thermal expansion behavior of the film is shown in figure 3(b). Shown also in the figure is the temperature dependence of lattice parameter of bulk Cu metal, as well as that of in-plane lattice parameter of the Cu film on MgO substrate, calculated from the assumption that in the in-plane direction, the expansion rate of the Cu film should be the same as that of the substrate material MgO. From this figure it is seen that the averaged out-of-plane expansion coefficient of the Cu film ( $24.1 \times 10^{-6}/\text{K}$  in 100~300 K) is much larger than that of Cu bulk ( $14.1 \times 10^{-6}/\text{K}$ ). This can be understood when one considers that the in-plane expansion of the Cu film is restricted by the substrate

which possesses a much lower thermal expansion coefficient ( $6.5 \times 10^{-6}/\text{K}$ ) in this temperature range.

Similarly, the clamping of FeNi alloy layers on the low expansion substrates could explain not only the larger thermal expansion of FeNi layers with Ni concentration of 54% (the bulk value for a corresponding alloy is about  $10 \times 10^{-6}/\text{K}$ ), but also the negative thermal expansion coefficient of the FeNi alloy layers with Ni concentration of 35% (shown in figure 2(b)). The negative expansion of Invar alloy layers in the out-of-plane direction is a result of the thermal expansion of substrate which is larger than that of the Invar alloy in this temperature range.

Based on the results above, one can conclude that typical Invar alloys with Ni concentrations around 35% have a low thermal expansion in 10~300 K, but the f. c. c. FeNi alloys of lower Ni concentrations, if

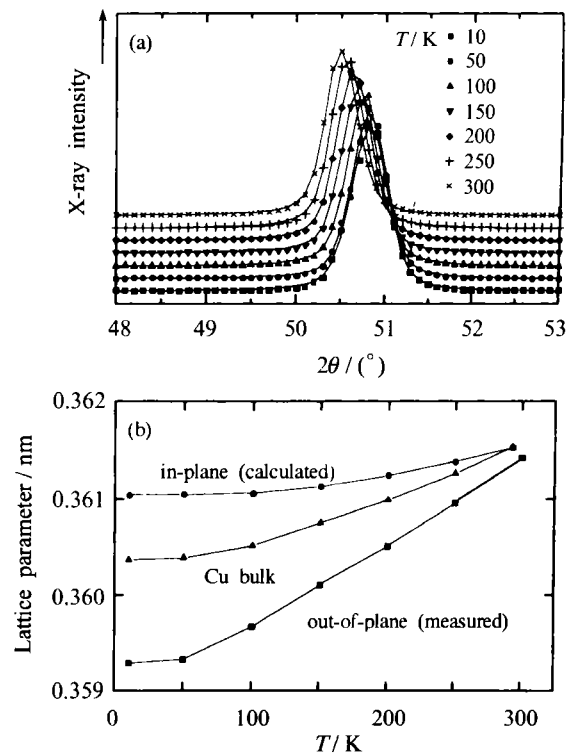


Figure 3 (a) X-ray diffraction peaks of a Cu epitaxial single layer at different temperatures. The curves have been displaced vertically for the reason of clarity. (b) Temperature dependence of out-of-plane (measured) and in-plane (calculated) lattice parameter of the Cu single layer, as well as that of bulk Cu metal

they can be stabilized until low temperatures, would show a relatively higher thermal expansion rate.

The explanation for the results above lies in the magnetic structure of the FeNi alloys. There exist

magnetic inhomogeneities in the low Ni alloy layers, that is, some small regions within the alloy are ferromagnetic, and the rest part of the alloy is nonferromagnetic due to fluctuations in composition [12]. When temperature rises, the alloy would show small abnormal contractions due to the fact that the nonferromagnetic regions should possess the anti-Invar behavior, in addition to the contraction related to the ferromagnetic regions within the alloys.

Magnetic measurements reveal that the FeNi alloy layers in the superlattices all show ferromagnetic behavior at room temperature. Figure 4 shows the temperature dependence of spontaneous magnetization of the three superlattices with different Ni concen-

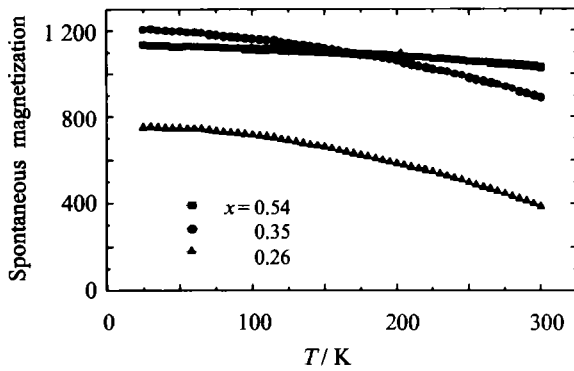


Figure 4 Temperature dependence of spontaneous magnetization for three  $\text{Fe}_{1-x}\text{Ni}_x/\text{Cu}$  superlattices

trations. It can be seen that among the three FeNi compositions shown in this figure, the 35% Ni Invar composition has the highest magnetization at low temperatures. On the other hand, the 26% Ni sample, which is of a composition well below the typical Invar composition, shows the lowest magnetization. This is consistent with the well-known deviation of magnetization from the Slater-Pauling curve found in FeNi bulk alloys [1].

As temperature increases, the magnetization of the Ni-richest sample ( $x = 54\%$ ) decreases gradually, while the Fe-richer samples show steeper declines in magnetization. The relative change in magnetization is the largest in the sample with FeNi alloy layers containing only 26% Ni, indicating that in this sample the ferromagnetic high-spin state of the FeNi alloy is energetically more adjacent to the paramagnetic low-spin state than in the Ni-richer samples [3].

Figure 5 shows room temperature magnetization curves of the superlattice of the lowest Ni content. It can be seen that the magnetization increases rather slowly with increasing magnetic field, seldom reach-

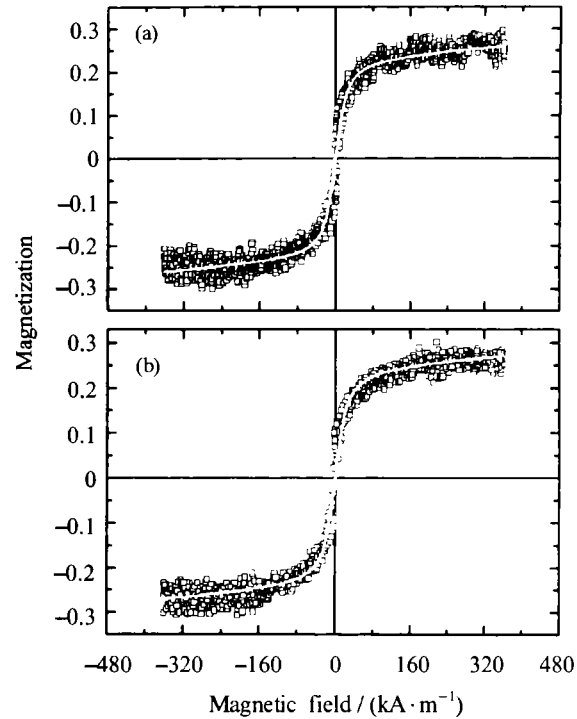


Figure 5 Magnetization curves of  $(\text{Fe}_{0.74}\text{Ni}_{0.26}/\text{Cu})_{10}$  superlattice at room temperature (points) in the in-plane [100] (a) and [110] (b) crystal directions, along with the fitted curves obtained by using the superparamagnetic model (the contral lines)

ing saturation in the highest magnetic field. Furthermore, there is no difference between the magnetization curves along the [100] and [110] crystal axes within the superlattice plane, reminding that the FeNi alloy in this sample is in a superparamagnetic state. Shown also in figure 5 are the fitted curves for magnetization based on the superparamagnetic model [13]:

$$M(H) = M_s \left[ \coth(\alpha) - \frac{1}{\alpha} \right] \quad (3)$$

where  $\alpha = mH/kT$ , and  $m$  is the magnetic moment of a superparamagnetic cluster in the alloy,  $H$  the magnetic field,  $T$  the temperature,  $k$  the Boltzmann's constant, and  $M_s$  the saturation magnetization of the ferromagnetic regions. From such fittings a magnetic moment  $m$  of  $3.8 \times 10^4$  Bohr magnetons is obtained, indicating that every ferromagnetic cluster in the FeNi layers would have  $3.8 \times 10^4$  atoms, corresponding to a small disk with an average diameter of about 7 nm (assuming that such a disk has a thickness of about 2.5 nm, the same as that of the FeNi sublayers), if it is assumed that every atom in the FeNi layers possess a magnetic moment of about 1 Bohr magneton [8].

The assumption of magnetic inhomogeneities has

been confirmed by recent experimental and theoretical investigations [12,14]. From such magnetic inhomogeneities, one would obtain not only a low spontaneous magnetization for low Ni alloys, but also a thermal expansion higher than the Invar alloy, since the thermal expansion should be an averaged behavior among volume fractions of both ferro- and nonferromagnetic states within the FeNi alloy layers.

### 3 Conclusions

With X-ray diffraction technique, the thermal expansion behaviors of FeNi alloy layers around the Invar composition have been investigated by using  $\text{Fe}_{1-x}\text{Ni}_x$ /Cu superlattice structures to stabilize the f. c. c. FeNi phase. In addition to the low thermal expansions of FeNi Invar alloy layers which can be expected from that of corresponding bulk materials, a large thermal expansion is observed for the alloy layers with lower Ni concentrations. It is believed that this rise in thermal expansion rate with the Ni content in the alloy decreasing is a result of magnetic inhomogeneities that exist in the FeNi layers of low Ni concentrations.

### References

- 1 E F Wassermann. *J Magn Magn Mater*, 1991, 100: 346
- 2 R J Weiss. *Proc Phys Soc*, 1963, 82: 281
- 3 V L Moruzzi. *Phys Rev B*, 1990, 41(10): 6939
- 4 E G Moroni, T Jarborg. *Phys Rev B*, 1990, 41(13): 9600
- 5 P Mohn, K Schwarz, D Wagner. *Phys Rev B*, 1991, 43(4): 3318
- 6 E Hoffmann, H Herper, P Entel, *et al.* *Phys Rev B*, 1993, 47(10): 5589
- 7 M Acet, T Schneider, H Zaehres, *et al.* *J Appl Phys*, 1994, 75(10): 7015
- 8 W Tang, Ch Gerhards, J Heise, *et al.* *J Appl Phys*, 1996, 80(4): 2327
- 9 E E Fullerton, I K Schuller, H Vanderstraeten, *et al.* *Phys Rev B*, 1992, 45(16): 9292
- 10 P Boedeker, A Abromeit, K Broehl, *et al.* *Phys Rev B*, 1993, 47(4): 2353~2361
- 11 C H MacGillavry, G D Rieck. *International Tables for X-ray Crystallography*, Vol. 3. Birmingham: The Kynoch Press, 1962. 201
- 12 J W Freeland, I L Grigorov, J C Walker. *J Appl Phys*, 1997, 81(8): 3897
- 13 C P Bean, I S Jacobs. *J Appl Phys*, 1956, 27(12): 1448
- 14 Y Wang, G M Stocks, D M C Nicholson, *et al.* *J Appl Phys*, 1997, 81(8): 3873

## Effect of the Solidification Conditions on the Microstructures of $\text{AlSi}_7\text{Mg}$ Alloy during Semi-solid Remelting

*Weimin Mao, Xueyou Zhong*

Material Science and Engineering School, University of Science and Technology Beijing, Beijing 100083, China

**Abstract:** The effect of the solidification conditions on the microstructures was studied during partial remelting of  $\text{AlSi}_7\text{Mg}$  alloy with the help of an electrical pipe-type furnace. The results show that the eutectic is remelted above all and  $\alpha$  phases are gradually evolved into spheroidal shape, if the  $\text{AlSi}_7\text{Mg}$  alloys stirred strongly by rotating electromagnetic field during the first solidification are heated again to 589 or 597°C and have been held for a short time (for example, 5~10 min), and moreover, the higher the holding temperature, the faster the eutectic remelting process and  $\alpha$  phase's evolution are. In contrast, even though the  $\text{AlSi}_7\text{Mg}$  alloy's samples non-stirred with fine dendritic microstructures are heated to the same temperatures as those stirred by rotating electromagnetic field and have been held for 60 min, it is not possible to change all the dendritic  $\alpha$  phases to spheroidal  $\alpha$  phase.

**Key words:**  $\text{AlSi}_7\text{Mg}$ ; remelting; electromagnetic stirring; dendrite

[From *Journal of University of Science and Technology Beijing (in Chinese)*, 1998, 20(3): 253]